Projected Antarctic extreme heat events in a warming world

Ariel Lena Morrison[1], Kyle Benjamin Heyblom[1], Hansi Alice Singh[1], and Philip J. Rasch[2]

[1]University of Victoria
[2]Pacific Northwest National Laboratory (DOE)

November 28, 2022

Abstract

As global temperatures increase, Antarctica is likely to experience increased frequency, duration, and intensity of extreme temperature events. Here we investigate how the characteristics of summer extreme temperature events - heatwaves and incidence of melt days - may change over Antarctica using daily historical and SSP5-8.5 Coupled Model Intercomparison Project phase 6 (CMIP6) output from 1950-2099. CMIP6 models robustly project that Antarctica's lowest elevation regions and the West Antarctic ice sheet will reach 0C for an average of 6-12 days during summer by 2099. Modelled summer heatwaves become more intense across the entire continent, but less frequent and shorter everywhere except the East Antarctic Plateau due to declining temperature variability as surface temperatures approach the melting point of ice. Our results imply that the increasing frequency of 0C days and greater heatwave intensity will contribute to increasing ice sheet surface melt and accelerating global sea level rise over the coming century.

Projected Antarctic extreme heat events in a warming world

A. L. Morrison[1], K. B. Heyblom[1], H. A. Singh[1], P. J. Rasch[2]

[1]School of Earth and Ocean Sciences, University of Victoria, Victoria, BC, Canada
[2]Department of Atmospheric Science, University of Washington, Seattle, WA, USA

Key Points:

- Average number of days with surface temperatures above 0°C over the WAIS projected to increase from 2 to 10 between 1951 and 2099
- Summer surface temperatures and heatwave intensity increase across entire Antarctic continent
- Heatwaves over ice sheets require new definition based on melting temperature and not on traditional baseline temperature threshold

Corresponding author: A. L. Morrison, `arielmorrison@uvic.ca`

Abstract

As global temperatures increase, Antarctica is likely to experience increased frequency, duration, and intensity of extreme temperature events. Here we investigate how the characteristics of summer extreme temperature events - heatwaves and incidence of melt days - may change over Antarctica using daily historical and SSP5-8.5 Coupled Model Intercomparison Project phase 6 (CMIP6) output from 1950-2099. CMIP6 models robustly project that Antarctica's lowest elevation regions and the West Antarctic ice sheet will reach 0°C for an average of 6-12 days during summer by 2099. Modelled summer heatwaves become more intense across the entire continent, but less frequent and shorter everywhere except the East Antarctic Plateau due to declining temperature variability as surface temperatures approach the melting point of ice. Our results imply that the increasing frequency of 0°C days and greater heatwave intensity will contribute to increasing ice sheet surface melt and accelerating global sea level rise over the coming century.

Plain Language Summary

Antarctica is an extremely cold, ice-covered continent, but it has already experienced record-breaking high temperatures - well above freezing - during the 2019/2020 summer. Days at or above freezing are a global concern because the Antarctic ice sheets contain enough water to increase global sea level by nearly 60 m (190 ft). Here we show that climate models project that the frequency and length of future summer heatwaves will increase in the middle of Antarctica and decrease closer to the coasts, but that the average temperature of heatwaves increases everywhere. Importantly for ice sheet stability, surface temperatures over Antarctica also reach the melting point for an average of 6-12 days during summer. This research suggests that Antarctica will keep warming in the future, but extreme summertime heat events only become more common in the middle of the continent. Even with shorter and less frequent heatwaves, however, the Antarctic ice sheet will continue to melt and affect global sea level because of the increase in melt days.

1 Introduction

Antarctica has warmed roughly 0.3°C decade^{-1} between 1950-2020 (Sato & Simmonds, 2021), though the warming trend is not homogeneous across the continent. West Antarctica, especially the Antarctic Peninsula, experienced a significant positive temperature trend between 1958-2016 (Gonzalez & Fortuny, 2018), associated with a variety of factors including warm marine air intrusions (Nicolas & Bromwich, 2011) and reductions in sea ice extent in the Amundsen and Bellingshausen Seas (Vaughan et al., 2003). East Antarctica, on the other hand, has had no observed annual temperature trend since 1958 (Nicolas & Bromwich, 2014). Notably, there has been a summertime cooling trend over East Antarctica (Hsu et al., 2021), partly due to ozone depletion and an associated positive trend in the Southern Annular Mode (SAM) during summer (Nicolas & Bromwich, 2014). Despite these opposing temperature trends, both sides of the continent experienced record-breaking high temperatures during the 2019/2020 summer season: ∼18°C at Esperanza Base on the Antarctic Peninsula and ∼9°C at Casey Station in East Antarctica (Robinson et al., 2020; Turner et al., 2021).

Extreme temperatures in Antarctica and the surrounding Southern Ocean are of both local and global concern. Locally, there are ecological impacts resulting from surface flooding (Barrett et al., 2008; Gooseff et al., 2017) and glacial retreat (Olech & Słaby, 2016) in response to extreme heat events, as well as surface albedo reductions from melting and refreezing snow (Jakobs et al., 2021) which can affect the rate of ice sheet melt. Globally, melting of the Antarctic ice sheet contributed roughly 0.27 mm yr^{-1} to the mean global sea level between 1993-2010 (Church et al., 2013). Continued melting and calving of the West Antarctic Ice Sheet (WAIS) in response to increasing ocean temperatures, especially in the summer, could raise sea level by up to 30 cm by 2100 (Seroussi et al., 2020) and by 3–5 m over the next 1000 years (Pan et al., 2021).

Prolonged exposure to warm air temperatures accelerates ice flow (Sugiyama et al., 2011), which can have a substantial impact on total ice sheet mass (Li et al., 2016). Extreme temperatures that persist for several days, or heatwaves, will likely contribute to increased melting and calving of the Antarctic ice sheet. Most work on Southern Hemisphere high latitude heatwaves has focused on marine heatwaves and their biological impacts (e.g., Plecha & Soares, 2020; Montie et al., 2020), or the ablation of ice sheets from below as the surrounding oceans warm (e.g., Alley et al., 2016). To our knowledge, no studies have assessed trends in future extreme heat events over the Antarctic continent. Given current and projected changes over the Antarctic Peninsula (AP) and WAIS (Joughin & Alley, 2011; Siegert et al., 2019), understanding the location, frequency, and intensity of future terrestrial extreme temperature events may be important in determining future Antarctic ice sheet mass loss.

In this study, we present the first analysis of future terrestrial Antarctic extreme temperature events in the Coupled Model Intercomparison Project Phase 6 (CMIP6; Eyring et al., 2016) climate models. We assess changes in regional and continent-wide summer heatwave intensity, frequency, and length, as well as occurrence of days with a maximum temperature at or above 0°C (melt days), over Antarctica from 1950-2099. Here we focus on differences in projected extreme heat events over the East Antarctic Plateau, the highest and driest region of Antarctica, and all other regions, particularly the AP and WAIS.

2 Data and Methods

2.1 Climate model data

This study uses daily near-surface maximum (T_{max}) and average (T_{avg}) temperature data from 29 CMIP6 Earth System Models (ESMs). For each ESM, we use up to 5 ensemble members, depending on availability. To avoid weighting our results towards models with more ensemble members, we calculate the multi-model mean using the mean of diagnosed extreme events from each ensemble member. We use historical experiment data from 1950-2014, and future climate projection data from 2015-2099. In order to assess the most extreme possibilities for Antarctic extreme heat events, all future projection data are from the SSP5-8.5, the future forcing scenario with the highest radiative forcing at the end of the century ($R_f = 8.5$ W m^{-2} at year 2100; see O'Neill et al., 2016). The selected CMIP6 models only include models that provided daily T_{max} and T_{avg} for historical and SSP5-8.5 experiments. Detailed information about each ESM's ensemble members and resolution is in the Supporting Information (Table S1).

2.2 Extreme heat event metrics and calculations

Following Perkins and Alexander (2013) and Perkins-Kirkpatrick and Lewis (2020), we define a heatwave as at least three consecutive days when daily T_{max} exceeds the 90th percentile of T_{max} for each calendar day. The 90th percentile is calculated from a rolling 15-day window of daily T_{max} from 1950-1979, with the window centered on the day in question (see the Supporting Information for an extended description of heatwave calculations). Using a fixed baseline for calculating heatwaves with the percentile method is common in heatwave studies (e.g., Dobricic et al., 2020; Hulley et al., 2020; Lyon et al., 2019; Plecha & Soares, 2020; Perkins & Fischer, 2013; Qui et al., 2021), and means that the temperature of each calendar day is compared against its own baseline. All temperature data from 1949-2099 are detrended with a third order polynomial fit prior to the threshold calculations and heatwave determinations. Without detrending, Antarctica is in near-perpetual summer heatwave conditions by 2099, as continent-wide mean warming exceeds the 90th percentile of the 1950-1979 temperature baseline threshold 29% of the 2099 summer.

We report three heatwave metrics: intensity, frequency, and duration. Intensity is the average heatwave temperature, frequency is the number of days under heatwave conditions, and duration is the length of the longest heatwave. Once a heatwave has been identified using the detrended daily T_{max} data, heatwave intensity is calculated using the true temperature (i.e., not detrended values) of the heatwave days. Since we are concerned with extreme temperatures over an ice sheet, we also determine how often Antarctic surface temperatures exceed 0°C, or the melting point of ice. Melt days are defined as days when T_{avg} exceeds 0°C. We report on the changing frequency of melt days as well as changes in heatwave metrics.

We focus on changes in summer (December-January-February; DJF) heatwave metrics and melt day frequency because the most extreme continent-wide temperatures have been recorded during summer. The summer season lasts 90 days in our analysis of each ESM, as all leap days (i.e., February 29) are removed to maintain consistency between models. Changes to summer heatwave metrics and melt day frequency are calculated between 1951-1980 and 2070-2099. Since each summer season spans two calendar years, the 1951 summer is December 1950 – February 1951, and the 1980 summer is December 1979 – February 1980.

3 Results

3.1 Antarctic temperature trends

Figure 1a shows the Antarctic regional and continent-wide trends in summer near-surface air temperature from 1951-2099. All regions experience a warming trend, with the greatest trend over the East Antarctic Plateau (EAP; temperatures increase by 0.7°C per decade from 2050 to 2099). The spatial pattern of warming is evident in Figure 1b, which shows the CMIP6 multi-model mean change in Antarctic summer near-surface air temperature between 1951-1980 and 2070-2099. There is a robust positive temperature

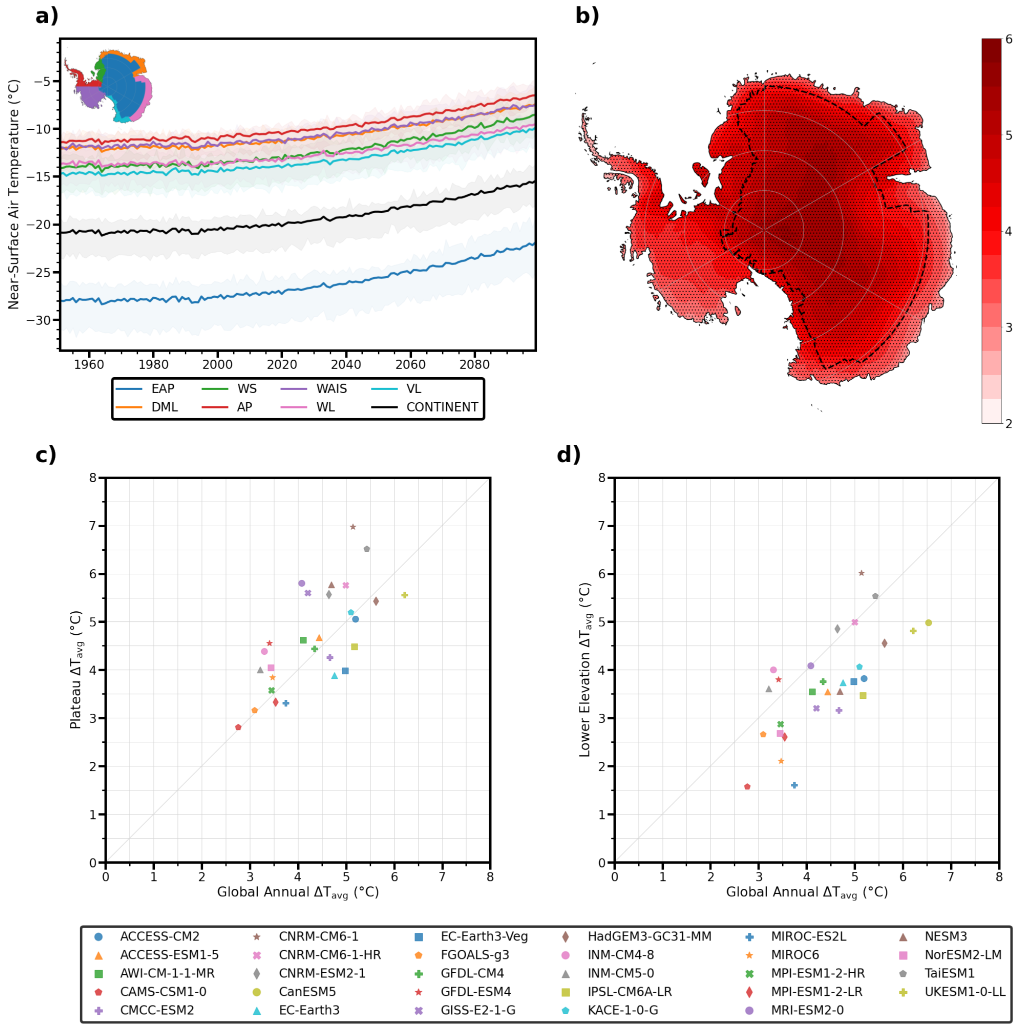

Figure 1. a) Trends in summer near-surface air temperature over the East Antarctic Plateau (EAP), Dronning Maud Land (DML), Weddell Sea (WS), Antarctic Peninsula (AP), West Antarctic Ice Sheet (WAIS), Wilkes Land (WL), Victoria Land (VL), and the entire continent from 1950-2099 in CMIP6-participating Earth System Models (ESMs). Regions are based on Thomas et al. (2017). We refer to all regions except for the EAP as 'lower elevation' regions. Solid lines are the CMIP6 multi-model mean; shading is the interquartile range around the mean. b) Change in CMIP6 multi-model mean near-surface air temperature during summer, 2070-2099 minus 1951-1980. Stippling indicates where ≥80% of the CMIP6 ESMs agree on the sign of the change. The contour line is the boundary between the lower elevation and EAP regions. c) Scatterplot of each CMIP6 ESM's change in daily summer T_{avg} over the EAP vs change in global annual mean T_{avg}, 2070-2099 minus 1951-1980. d) As in (c) except over the lower elevation regions of Antarctica.

trend across the entire continent, and the entire Antarctic continent warms in every ESM examined here (Fig 1b; note that stippling indicates that ≥80% of CMIP6 models agree on the sign of the temperature change at that location; also see Fig. S1). The contour line separates the EAP from the remaining regions. Since the EAP region is defined and characterized by its high elevation, we group and refer to all regions except the EAP as 'lower elevation' regions in this study. The entire continent warms by at least 2°C, but the largest changes are over the central EAP, which sees an increase of nearly 6°C over 150 years in the multi-model mean. The Antarctic Peninsula (AP) and West Antarctic Ice Sheet (WAIS) each experience a smaller temperature increase of nearly 5°C. Regional differences in warming are again apparent when comparing summer season warming over the EAP (Fig. 1c) and over the lower elevation regions (Fig. 1d) with the change in annual global mean surface warming in each ESM: in most models, EAP warming is greater than the annual mean global warming, but mean lower elevation regional warming is weaker than annual mean global warming in most models. Even though the EAP is the coldest region of Antarctica (Fig. 1a), it warms faster than the global mean in all models, a finding consistent with the significant South Pole warming in Clem et al. (2020).

3.2 Changes to extreme temperature events

We have shown that Antarctic mean temperatures robustly warm over the 21st century in all CMIP6-participating ESMs in this study (Fig. 1, Fig. S1). We next assess changes in temperature extremes. Figure 2 shows projected changes in heatwave characteristics: intensity, frequency, and duration. Heatwave intensity, the average heatwave temperature over a given time period, increases over nearly the entire continent (Fig 2a). However, the intensity of heatwaves does not increase uniformly over all regions (Fig. 2a; see also Fig. S2): as with the average increase in surface temperature (recall Fig. 1a), heatwave intensity increases most over the EAP. In the CMIP6 multi-model mean, increased heatwave intensity is robust everywhere except parts of the WAIS and AP (Fig. 2b). Over the EAP, heatwave intensity in an individual ESM has a nearly one-to-one relationship with the mean surface temperature change in that ESM (correlation coefficient = 0.91 and slope = 0.85°C °C^{-1}; Fig. S3a), while the change in lower elevation heatwave intensity in an ESM is always less than the mean surface temperature change in that ESM (Fig. S3b).

Unlike near-surface temperature and heatwave intensity, heatwave frequency (number of days under heatwave conditions; Figs. 2c, 2d) and duration (length of longest heatwave; Figs. 2e, 2f) do not increase across all of Antarctica. Frequency and duration decrease in all lower elevation regions from 1951-2099, with a modest increase over the central EAP. However, only the lower elevation decline in frequency and duration is robust across the ESMs. The largest declines are over the AP and WAIS, indicating that Western Antarctica may see up to six fewer days under heatwave conditions at the end of the 21st century, and the longest duration of heatwaves that do occur may be up to four days shorter. While the lower elevation declines in heatwave frequency and length are robust in the CMIP6 multi-model mean, ESMs agree on neither the magnitude nor direction of change over the EAP (Figs. S4, S5). For example, MRI-ES2-0 projects a nearly 15-day increase in heatwave days in the center of the EAP, while ACCESS-CM2 projects a 5-day decrease in heatwave days over this same region.

While CMIP6-participating ESMs robustly project that Antarctica will warm everywhere, the Antarctic continent is still very cold in 2099; the average projected 2099 summer surface temperature in the CMIP6 multi-model mean is roughly -15°C, still well below freezing. As an ice sheet, Antarctica is particularly sensitive to the temperature threshold of 0°C, the melting point of ice. We find a robust increase in the number of summer days when T_{avg} exceeds 0°C (i.e., melt days; Fig. 3a), even though average summer temperatures do not consistently reach the melting point (0°C) in the multi-model mean (Fig. 1a). The regional mean heatwave intensity also does not reach 0°C in the

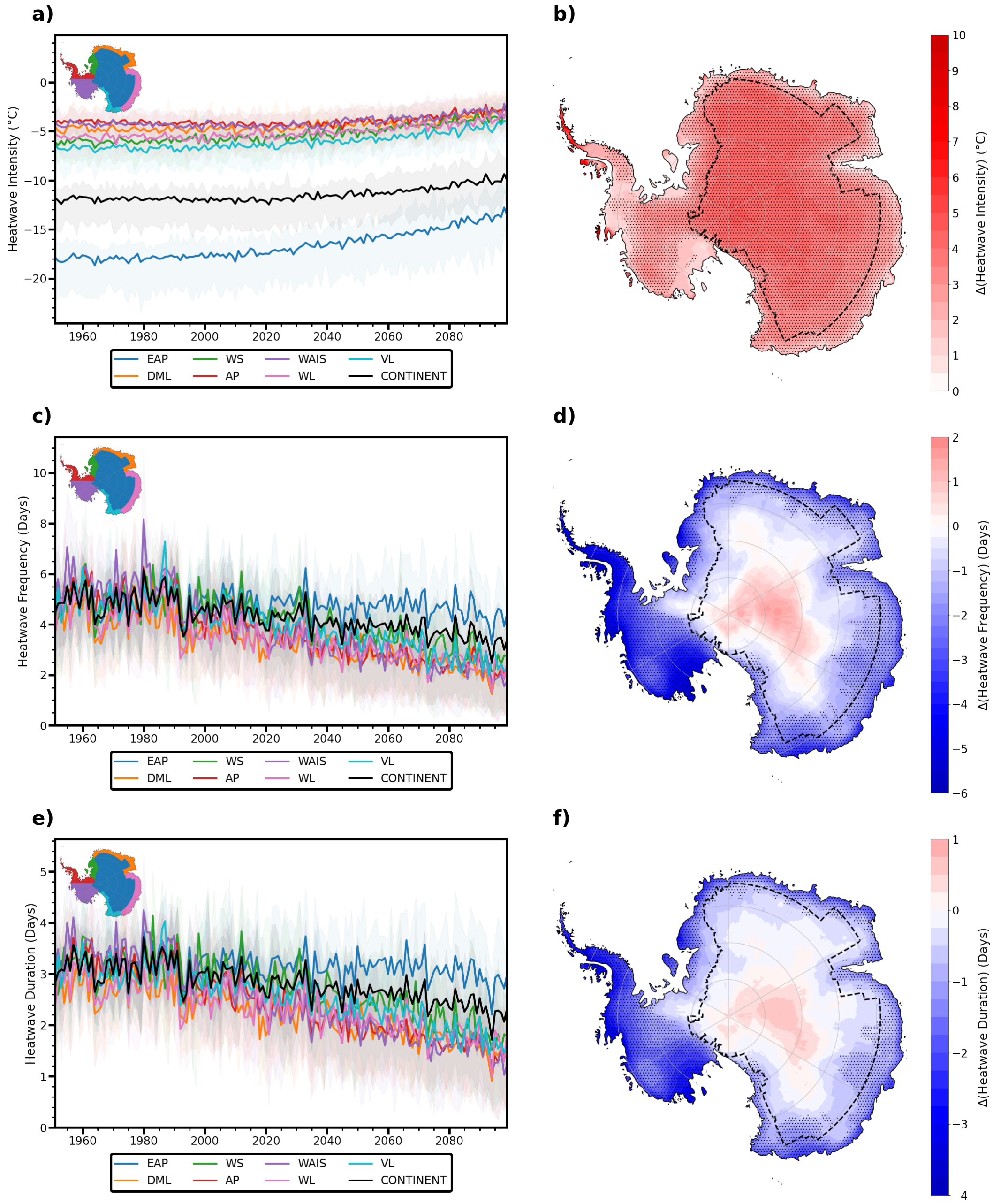

Figure 2. a) Trends in regional and continent-wide summer heatwave intensity from 1951-2099. Solid lines are the CMIP6 multi-model mean; shading is the interquartile range around the mean. b) Change in CMIP6 multi-model mean summer heatwave intensity (in °C), 2070-2099 minus 1951-1980. Stippling indicates where ≥80% of the CMIP6 models agree on the sign of the change. The contour line is the boundary between EAP and lower elevation regions. c) As in (a) except for heatwave frequency (in days per summer season). d) As in (b) except for heatwave frequency. e) As in (a) except for heatwave length (i.e., the length in days of the longest heatwave). f) As in (b) except for heatwave length.

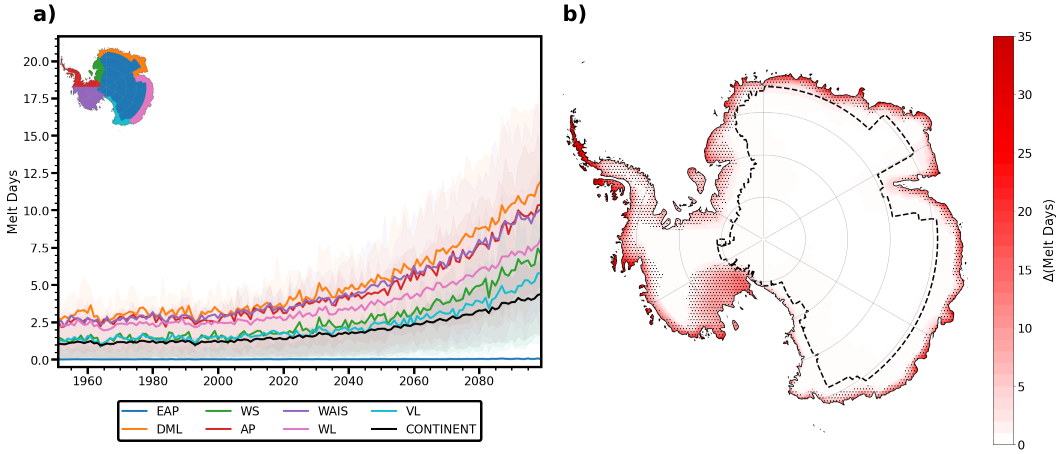

Figure 3. a) Regional and continent-wide trends in the number of days where daily T_{avg} exceeds 0°C (melt days). Solid lines are the CMIP6 multi-model mean and shading is the interquartile range around the mean. b) Change in CMIP6 multi-model mean melt day frequency, 2070-2099 minus 1951-1980. Stippling indicates where ≥80% of the CMIP6 models agree on the sign of the change. The contour line is the boundary between EAP and lower elevation regions.

CMIP6 multi-model mean (Fig. 2a), indicating that the melting point always exceeds the 90th percentile of summertime T_{max} (though intensity may reach 0°C over individual grid cells, especially over lower elevation coastal regions). From 1951-2099, there is an increase in melt days over every lower elevation region. The largest number of melt days occur over the AP, WAIS, and Dronning Maud Land (DML). The EAP is the only region with no projected melt days. The change in melt day frequency over the lower elevation regions is robust across ESMs (Fig. 3b; also see Fig. S6): all lower elevation regions will, on average, see an increase of 4-9 melt days by 2099. In other words, models project that the entire Antarctic coast and the WAIS may experience surface melt for almost 10% of the summer by 2099.

3.3 Changes in summer surface temperature variability

To understand why there is a robust increase in melt days over Antarctica in the CMIP6 multi-model ensemble, but not a robust increase in heatwave persistence metrics (i.e., frequency and duration), we examine the change in summer season daily temperature variability. Temperature variability decreases over much of Antarctica as it warms: in the CMIP6 multi-model mean, the standard deviation of daily summer T_{max} decreases by up to 1.3°C in lower elevation regions, with the largest decreases over the AP and WAIS (see Fig. 4a; see also Fig. S7). Declining variability over the lower elevation regions is connected to the increase in melt days (Fig. 4b): the inter-model spread in melt day increase (Fig. S6) is inversely correlated with the inter-model spread in declining variability (Fig. S7). That is, models with the largest projected increase in melt days over a particular grid cell also have the greatest projected decline in temperature variability over the same grid cell.

The probability distribution functions (PDFs) of daily near-surface temperatures over the EAP (Fig. 4c) and lower elevation regions (Fig. 4d) clearly show declining temperature variability over the latter between 2070-2099 (green) compared to 1951-1980 (black). To illustrate this declining temperature variability, we shift the 2070-2099 temperature distribution such that the means of each PDF are overlapped (gray dotted line; note the green and black x-axes corresponding to 2070-2099 and 1951-1980, respectively).

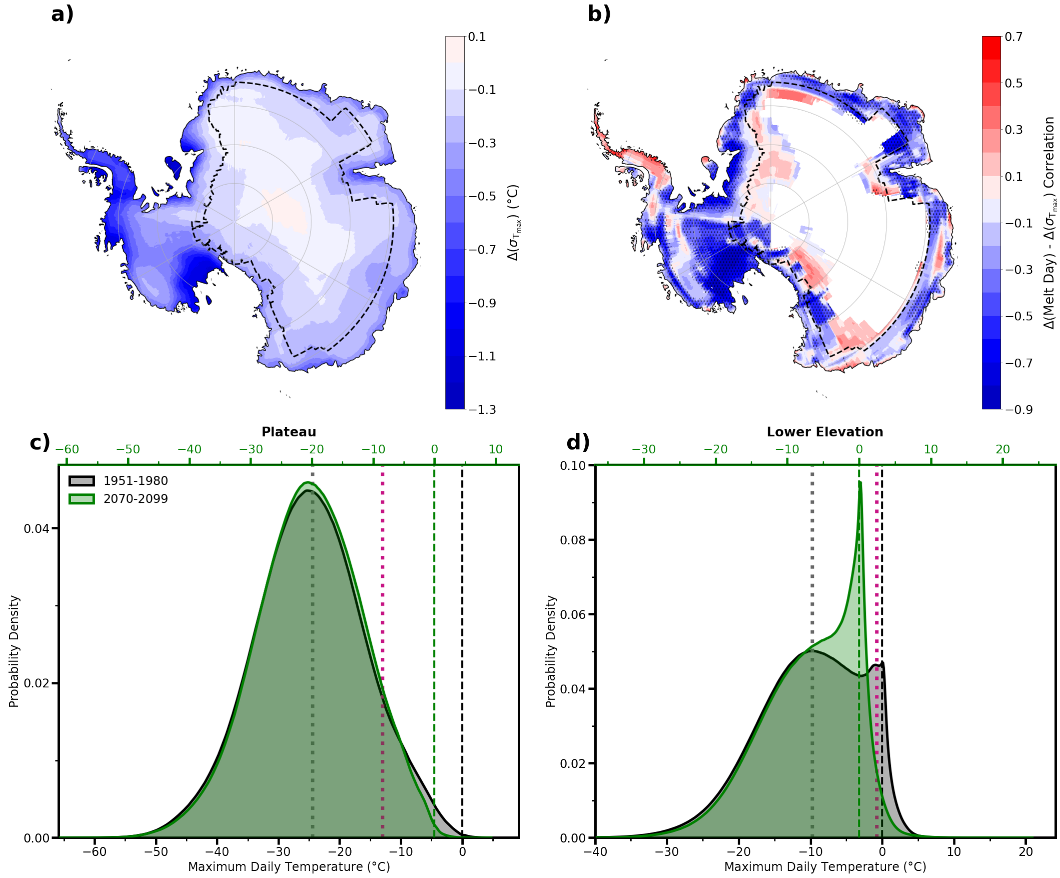

Figure 4. a) CMIP6 multi-model mean change in the standard deviation of daily summer T_{max}, 2070-2099 minus 1951-1980. b) Pearson correlation between the CMIP6 multi-model mean change in standard deviation of daily summer T_{max} (a) with the change in number of melt days (Fig. 3b). Stippling indicates where $p < 0.05$. The contour line in (a) and (b) is the boundary between EAP and lower elevation regions. c) CMIP6 multi-model pooled probability distribution function (PDF) of the summer daily summer T_{max} over the East Antarctic Plateau (EAP) during 1951-1980 (black) and 2070-2099 (green). Note the different x-axes for each time period. Both PDFs are overlapped so that the mean T_{max} falls on the same gray dotted line. The magenta dotted line is the 90^{th} percentile of T_{max} during 1951-1980. The black (green) dashed line is the 0°C threshold during 1951-1980 (2070-2099). d) As in (c) except for lower elevation regions.

When the means overlap, we see that the tail of the 2070-2099 PDF is narrower than the 1951-1980 PDF. Importantly, shifting the PDFs also allows us to visualize where the temperature distributions fall with respect to the 90$^{\mathrm{th}}$ percentile of T_{max} during 1951-1980 (magenta dotted lines in Figs. 4c and 4d, which provide a visual representation of the temperature threshold used for heatwave calculations; see also Fig. S8). The temperature threshold for a heatwave over the baseline period is just below 0°C in the lower elevation regions (black dashed line, Fig. 4d), indicating that the daily temperature over a lower elevation grid cell must reach or exceed the melting point to be considered part of a heatwave at this time. Over 2070-2099, on the other hand, this temperature threshold is > 2°C, well over the melting point.

The melting point is an important physical constraint on near-surface temperatures over an ice sheet. Grid cells do reach the 0°C threshold by 2070-2099 (green dashed line, Figs. 4c, 4d), but cannot exceed it significantly because they are limited by the melting point of the ice at the surface. As a result of this physical constraint, temperature variability declines because the upper tail of the 2070-2099 PDF shortens such that near-surface temperatures do not exceed the melting temperature most of the time. In 2070-2099, this means that daily temperatures are less likely to exceed the 90$^{\mathrm{th}}$ percentile temperature threshold from the baseline period. As a result, heatwave frequency and duration decline.

4 Discussion

Our results show that Antarctica robustly warms through the 21$^{\mathrm{st}}$ century (Fig. 1; Fig. S1), leading to a robust increase in the number of melt days (Fig. 3; Fig. S6). Melt days only occur over the lower elevation regions of Antarctica, not over the high and dry EAP. All lower elevation regions have a warmer baseline than the EAP (Fig. 1a), so any warming brings them closer to the melting threshold. Heatwave intensity also increases over the entire continent (Fig. 2b), and is robust everywhere except parts of the WAIS and AP.

The projected increase in melt days is related to two unexpected results of this study: declining heatwave frequency and duration over the lower elevation regions (Fig. 2). Surface air temperatures over ice sheets are limited to or just above the melting point, reflecting fundamental physical constraints on surface air temperature over underlying ice. Skin temperature over an ice sheet does not exceed the melting point until the ice is gone. That the lower elevation temperatures in some CMIP6 ESMs do exceed the melting point (Fig. S8) is because we use near-surface air temperatures, and not skin temperature, to calculate heatwave and melt day metrics. Near-surface temperature variability decreases as more of the coastal and West Antarctica ice sheets melt (Fig. 4a), constraining surface temperatures over many lower elevation grid cells to approximately 0°C. As temperature variability decreases, the tail of the temperature distribution shortens (Fig. 4d), decreasing the likelihood of climatologically extreme temperatures. As a result, heatwaves become less frequent and shorter as temperature variability decreases. This reasoning is similar to that of Argüeso et al. (2016), who found that projected declines in temperature variability over Greenland and Antarctica narrowed the temperature distribution and could result in decreased heatwave frequency and duration, even as the mean temperature increases.

The declines in lower elevation heatwave frequency and duration are not physically meaningful in regards to future projections of Antarctic ice sheet mass loss. That is, we cannot interpret shorter and less frequent heatwaves to mean that Antarctica will be less vulnerable to ice sheet melt. Increasing surface temperatures (Fig. 1), heatwave intensity (Fig. 2a, 2b), and melt day frequency (Fig. 3) will increase the speed at which Antarctic ice sheets flow and lose mass. CMIP6 models robustly project that Thwaites Glacier, a rapidly retreating glacier (Scambos et al., 2017, and references therein) which falls within the WAIS region of our study, could experience 15 days of melt by the end of this century - an increase of 10 days from the present climate. The Ross Ice Shelf, located in the bay between the WAIS and Victoria Land (VL) regions, is projected to lose roughly 40% of its mass by 2099 (Naughten et al., 2018) and reveal open ocean during summer. Onshore advection of warmer marine air is a possible cause of the robust increase in melt days projected over the WAIS west of the Ross Ice Shelf (recall Fig. 3b). Increasing melt day frequency can substantially affect ice sheet dynamics. For example, freeze-thaw cycles on the surface of the Greenland Ice Sheet (GIS) can open cracks through which meltwater drains, lubricating the base of the glacier and speeding up glacier flow (Phillips et al., 2013), while melting the surface of Antarctica can affect ice shelf stability (Trusel et al., 2012). Given the physical effects of increasing melt days, changes in melt day frequency may be a more relevant metric for assessing the impact of extreme heat events on ice sheets than considering the effect of heatwaves.

Placing our results within the broader context of heatwave studies may be difficult because of Antarctica's unique location and geography. Most heatwave studies have focused on the northern mid-latitudes because of heatwaves' impacts on human health. Projected declines in Antarctic summer heatwave frequency and duration are opposite to common results over the mid-latitudes and tropics. Over North America and Europe, heatwaves are projected to increase in frequency and duration (Field et al., 2012; Horton et al., 2016). Increases in mid-latitude heatwaves have been attributed in part to low soil moisture (Miralles et al., 2014; Zampieri et al., 2009) from rising temperatures; low soil moisture in turn reduces latent heat flux out of the ground, which causes a positive feedback that further increases temperature. Soil moisture is unrelated to changes in Antarctic heatwave metrics, however, since Antarctic heatwaves occur over an ice sheet. On the other hand, factors controlling Antarctic temperature extremes are likely related to those controlling temperature extremes over the GIS. Observed heatwaves over Greenland have been linked to sea ice melt (Dobricic et al., 2020), increasing moisture transport from atmospheric river events (Mattingly et al., 2018; W et al., 2014), and liquid-containing clouds (Bennartz et al., 2013). While a full assessment of the atmospheric conditions linked to Antarctic heatwaves is outside the scope of this paper, it is likely that clouds and atmospheric moisture transport also play a role in Antarctic heatwave intensity, frequency, and duration.

Assessing extreme heat events over ice sheets or at the high latitudes may require a different definition of 'heatwave' than used in mid-latitude studies. Ice sheets are most strongly affected by temperatures exceeding a specific threshold: 0°C. While all warming over an ice sheet affects ice rheology, reaching the melting point can cause rapid surface ablation. Surface temperature over an ice sheet will also remain at the melting point until the ice is gone, so temperatures will not continue rising and heatwaves, as traditionally defined, will become less frequent and shorter. We therefore propose that heatwaves over ice be assessed in the context of the melting temperature and not in the context of exceeding a historical baseline (i.e., a common definition for mid-latitude heatwaves or marine heatwaves).

5 Conclusions

In this study, we have assessed daily historical and SSP5-8.5 temperature data from 29 CMIP6 models to determine how summer heatwaves and frequency of melt days over continental Antarctica may change through the 21st century. Heatwaves will likely become more intense (i.e., higher average temperature) over the entire continent, with the largest increase of ∼4°C over the central East Antarctic Plateau. Both the frequency (number of days under heatwave conditions) and duration (length of longest heatwave) robustly decrease over the lower elevation regions of Antarctica due to declining surface temperature variability. Declining temperature variability in turn is highly correlated ($p < 0.05$) with a robust increase in melt day frequency over lower elevation regions, notably over the vulnerable regions of the WAIS. The likelihood of exceeding the heatwave temperature threshold decreases with more melt days because the melting temperature of ice acts as a physical constraint on further increasing temperatures over an ice sheet. Based on these results, we believe that heatwaves over ice sheets should be assessed in the context of melt days instead of being compared to a baseline temperature distribution. Our results suggest that the increase in melt days will substantially alter the surface mass balance over lower elevation regions of Antarctica, even though heatwaves become less common and shorter over the next 80 years.

6 Open Research

The daily CMIP6 data used for calculating extreme heat event metrics are publicly available after free registration through the World Climate Research Programme CMIP6 website (https://esgf-node.llnl.gov/search/cmip6/).

Acknowledgments

ALM and PJR were supported by the Regional and Global Model Analysis (RGMA) program of the U.S. Department of Energy's Office of Science as a contribution to the Hi-LAT project. HAS, KH, and ALM were supported by the University of Victoria. This research also used computing resources at the University of Victoria. The authors declare no competing interests.

References

Alley, K. E., Scambos, T. A., Siegfried, M. R., & Fricker, H. A. (2016). Impacts of warm water on antarctic ice shelf stability through basal channel formation. *Nature Geoscience*, *9*, 290–293.

Argüeso, D., Di Luca, A., Perkins-Kirkpatrich, S., & Evans, J. P. (2016). Seasonal mean temperature changes control future heat waves. *Geophysical Research Letters*, *43*, 7653–7660. doi: 10.1002/2016GL069408

Barrett, J. E., Virginia, R. A., Wall, D. H., Doran, P. T., Fountain, A. G., Welch, K. A., & Lyons, W. B. (2008). Persistent effects of a discrete warming event on a polar desert ecosystem. *Global Change Biology*, *14*(10), 2249–2261.

Bennartz, R., Shupe, M. D., Turner, D. D., Walden, V. P., Steffen, K., Cox, C. J., . . . Pettersen, C. (2013). July 2012 greenland melt extent enhanced by low-level liquid clouds. *Nature*, *496*, 83–86.

Church, J. A., Clark, P. U., Cazenave, A., Gregroy, J. M., Jevrejeva, S., Levermann, A., . . . Unnikrishnan, A. S. (2013). Sea level change. *Climate Change 2013: The Physical Science Basis. Contribution of Working Group I to the Fifth Assessment Report of the Intergovernmental Panel on Climate Change*, [Stocker, T.F., D. Qin, G.-K. Plattner, M. Tignor, S.K. Allen, J. Boschung, A. Nauels, Y. Xia, V. Bex and P.M. Midgley(eds.)]. Cambridge University Press, Cambridge, United Kingdom and New York, NY, USA.

Clem, K. R., Fogt, R. L., Turner, J., Lintner, B. R., Marshall, G. J., Miller, J. R., & Renwick, J. A. (2020). Record warming at the south pole during the past three decades. *Nature Climate Change*, *10*, 762-770.

Dobricic, S., Russo, S., Pozzoli, L., Wilson, J., & Vignati, E. (2020). Increasing occurrence of heat waves in the terrestrial arctic. *Environmental Research Letters*, *15*(2), 024022.

Eyring, V., Bony, S., A, M. G., Senior, C. A., Stevens, B., Stouffer, R. J., & Taylor, K. E. (2016). Overview of the coupled model intercomparison project phase 6 (cmip6) experimental design and organization. *Geoscientific Model Development*, *9*, 1937–1958.

Field, C. B., Barros, V., Stocker, T. F., Qin, D., Dokken, D. J., Ebi, K. L., . . . Midgley, P. M. (2012). Managing the risks of extreme events and disasters to advance climate change adaptation. *A Special Report of Working Groups I and II of the Intergovernmental Panel on Climate Change*, 231–290. Cambridge University Press, Cambridge, United Kingdom and New York, NY, USA.

Gonzalez, S., & Fortuny, D. (2018). How robust are the temperature trends on the antarctic peninsula? *Antarctic Science*, *30*(5), 322–328.

Gooseff, M. N., Barrett, J. E., Adams, B. J., Doran, P. T., Fountain, A. G., Lyons, W. B., . . . Wall, D. H. (2017). Decadal ecosystem response to an anomalous melt season in a polar desert in antarctica. *Nature Ecology Evolution*, *1*(9), 1334–1338.

Horton, R. M., Mankin, J. S., Lesk, C., Coffel, E., & Raymond, C. (2016). A review of recent advances in research on extreme heat events. *Current Climate Change Reports*, *2*, 242–259. doi: 10.1007/s40641-016-0042-x

Hsu, P.-C., Fu, Z., Murakami, H., Lee, J.-Y., Yoo, C., Johnson, N. C., ... Liu, Y. (2021). East antarctic cooling induced by decadal changes in madden-julian oscillation during austral summer. *Science Advances*, *7*, eabf9903.

Hulley, G. C., Dousset, B., & Kahn, B. H. (2020). Rising trends in heatwave metrics across southern california. *Earth's Future*, *8*(7), e2020EF001480.

Jakobs, C. L., Reijmer, C. H., van den Broeke, M. R., van de Berg, W. J., & van Wessem, J. M. (2021). Spatial variability of the snowmelt-albedo feedback in antarctica. *Journal of Geophysical Research: Earth Surface*, *126*, e2020JF005696.

Joughin, I., & Alley, R. B. (2011). Stability of the west antarctic ice sheet in a warming world. *Nature Geoscience*, *4*(8), 506-513.

Li, X., Rignot, E., Mouginot, J., & Scheuchl, B. (2016). Ice flow dynamics and mass loss of totten glacier, east antarctica, from 1989 to 2015. *Geophysical Research Letters*, *43*, 6366–6373.

Lyon, B., Barnston, A. G., Coffel, E., & Horton, R. M. (2019). Projected increase in the spatial extent of contiguous us summer heat waves and associated attributes. *Environmental Research Letters*, *14*(11), 114029.

Mattingly, K. S., Mote, T. L., & Fettweis, X. (2018). Atmospheric river impacts on greenland ice sheet surface mass balance. *Journal of Geophysical Research: Atmospheres*, *123*(16), 8538–8560. doi: 10.1029/2018JD028714

Miralles, D. G., Teuling, A. J., van Heerwaarde, C. C., & Vilá-Guerau de Arellano, J. (2014). Mega-heatwave temperatures due to combined soil desiccation and atmospheric heat accumulation. *Nature Geoscience*, *7*, 345–349.

Montie, S., Thomsen, M. S., Rack, W., & Broady, P. A. (2020). Extreme summer marine heatwaves increase chlorophyll a in the southern ocean. *Antarctic Science*, *32*(6), 508-509.

Naughten, K. A., Meissner, K. J., Galton-Fenzi, B. K., England, M. H., Timmermann, R., & Hellmer, H. H. (2018). Future projections of antarctic ice shelf melting based on cmip6 projections. *Journal of Climate*, *31*(13), 5243–5261. doi: 10.1175/JCLI-D-17-0854.1

Nicolas, J. P., & Bromwich, D. H. (2011). Climate of west antarctica and influence of marine air intrusions. *Journal of Climate*, *24*(1), 49–67.

Nicolas, J. P., & Bromwich, D. H. (2014). New reconstruction of antarctic near-surface temperatures: Multidecadal trends and reliability of global reanalyses. *Journal of Climate*, *27*(21), 8070–8093.

Olech, M., & Słaby, A. (2016). Changes in the lichen biota of the lions rump area, king george island, antarctica, over the last 20 years. *Polar Biology*, *39*, 1499–1503.

O'Neill, B. C., Tebaldi, C., van Vuuren, D. P., Eyring, V., Friedlingstein, P., Hurtt, G., ... Sanderson, B. M. (2016). The scenario model intercomparison project (scenariomip) for cmip6. *Geoscientific Model Development*, *9*, 3461–3482.

Pan, L., Powell, E. M., Latychev, K., Mitrovica, J. X., Creveling, J. R., Gomez, N., ... Clark, P. U. (2021). Rapid postglacial rebound amplifies global sea level rise following west antarctic ice sheet collapse. *Science Advances*, *7*, eabf7787.

Perkins, S. E., & Alexander, L. V. (2013). On the measurement of heat waves. *Journal of Climate*, *26*, 4500–4517.

Perkins, S. E., & Fischer, E. M. (2013). The usefulness of different realizations for the model evaluation of regional trends in heat waves. *Geophysical Research Letters*, *20*(21), 5793-5797.

Perkins-Kirkpatrick, S., & Lewis, S. (2020). Increasing trends in regional heatwaves. *Nature Communications*, *11*(1), 1–8.
Phillips, T., Rajaram, H., Colgan, W., Steffen, K., & Abdalati, W. (2013). Evaluation of cryo-hydrologic warming as an explanation for increased ice velocities in the wet snow zone, sermeq avannarleq, west greenland. *Journal of Geophysical Research: Earth Surface*, *118*, 1241–1256. doi: 10.1002/jgrf.20079
Plecha, S. M., & Soares, P. M. M. (2020). Global marine heatwave events using the new cmip6 multi-model ensemble: from shortcomings in present climate to future projections. *Environmental Research Letters*, *15*(12), 124058.
Qui, Z., Qiao, F., Jan, C. J., Zhang, L., & Song, Z. (2021). Evaluation and projection of global marine heatwaves based on cmip6 models. *Deep-Sea Research Part II: Topical Studies in Oceanography*, *194*(6), 104998.
Robinson, S. A., Klekociuk, A. R., King, D. H., P, R. M., Zúñiga, G. E., & Bergstrom, D. M. (2020). The 2019/2020 summer of antarctic heatwaves. *Global Change Biology*, *26*(6), 3178–3180.
Sato, K., & Simmonds, I. (2021). Antarctic skin temperature warming related to enhanced downward longwave radiation associated with increased atmospheric advection of moisture and temperature. *Environmental Research Letters*, *16*(6), 064059.
Scambos, T. A., Bell, R. E., Alley, R. B., Anandakrishnan, S., Bromwich, D. H., Brunt, K., … Yager, P. L. (2017). How much, how fast?: A science review and outlook for research on the instability of antarctica's thwaites glacier in the 21st century. *Global and Planetary Change*, *153*, 16–34.
Seroussi, H., S, N., Payne, A. J., Goelzer, H., Lipscomb, W. H., Abe-Ouchi, A., … ... Zwinger, T. (2020). Ismip6 antarctica: a multi-model ensemble of the antarctic ice sheet evolution over the 21st century. *The Cryosphere*, *14*, 3033–3070. doi: 10.5194/tc-14-3033-2020
Siegert, M., Atkinson, A., Banwell, A., Brandon, M., Convey, P., Davies, B., … Vaughan, D. (2019). The antarctic peninsula under a 1.5°c global warming scenario. *Frontiers in Environmental Science*, *7*, 1–7.
Sugiyama, S., Skvarca, P., Naito, N., Enomoto, H., Tsutaki, S., Tone, K., … Aniya, M. (2011). Ice speed of a calving glacier modulated by small fluctuations in basal water pressure. *Nature Geoscience*, *4*, 597–600.
Thomas, E. R., van Wessem, J. M., Roberts, J., Isaksson, E., Schlosser, E., Fudge, T. J., … Ekaykin, A. A. (2017). Regional antarctic snow accumulation over the past 1000 years. *Climate of the Past*, *13*, 1491-1513.
Trusel, L. D., Frey, K. E., & Das, S. B. (2012). Antarctic surface melting dynamics: Enhanced perspectives from radar scatterometer data. *Journal of Geophysical Research*, *117*, F02023. doi: 10.1029/2011JF002126
Turner, J., Lu, H., King, J., J, M. G., Phillips, T., Bannister, D., & Colwell, S. (2021). Extreme temperatures in the antarctic. *Journal of Climate*, *34*(7), 2653–2668.
Vaughan, D. G., Marshall, G. J., Connolley, W. M., Parkinson, C., Mulvaney, R., Hodgson, D. A., … Turner, J. (2003). Recent rapid regional climate warming on the antarctic peninsula. *Climatic Change*, *60*(3), 243-274.
W, N., P, C. G., M, R. F., & D, S. M. (2014). Continental heat anomalies and the extreme melting of the greenland ice surface in 2012 and 1889. *Journal of Geophysical Research: Atmospheres*, *119*, 6520—6536.
Zampieri, M., D'Andrea, F., Vautard, R., Ciais, P., de Noblet-Ducoudré, N., & Yiou, P. (2009). Hot european summers and the role of soil moisture in the propagation of mediterranean drought. *Journal of Climate*, *22*, 4747–4758. doi: 10.1175/2009JCLI2568.1

Supporting Information for "Projected Antarctic extreme heat events in a warming world"

A. L. Morrison[1], K. Heyblom[1], H. A. Singh[1], P. J. Rasch[2]

[1]School of Earth and Ocean Sciences, University of Victoria, Victoria, BC, Canada

[2]Department of Atmospheric Science, University of Washington, Seattle, WA, USA

Contents of this file

Introduction The supporting information contains a more detailed description the heatwave calculations made in this study (Text S1), a table for ensemble members and horizontal resolution of the CMIP6 models used in this study (Table S1), and additional figures (S1 to S8). These figures show results for each CMIP6 model, while the figures in the main text show results for the CMIP6 multi-model mean.

Text S1.

Corresponding author: A. L. Morrison, School of Earth and Ocean Sciences, University of Victoria, Bob Wright Centre, Victoria, BC V8P 5C2, Canada. (arielmorrison@uvic.ca)

We used the following steps to determine whether a day experiences a heatwave:

1. Any models with leap years have all February 29th days removed.

2. T_{max} from 1949–2099 is detrended by fitting a third order polynomial least squares fit and subtracting this trend from the entire time period.

3. Heatwave thresholds are determined for each day of the year by calculating the 90th percentile of T_{max} within a 15-day rolling window. Using a rolling window captures the time dependence of surface temperature. The 15-day rolling window is centered on the day being evaluated, for all years over the period from 1950–1979 of the detrended T_{max} values. For example, the threshold for January 8th is evaluated as the 90th percentile T_{max} of all days from January 1st to January 15th from 1950–1979 (a total of 450 days).

4. A separate threshold is determined for each ensemble member, each calendar day (i.e., if a model uses a 365 day calendar, 365 thresholds are determined), and for each grid box over Antarctica.

5. A day experiences a heatwave if the detrended T_{max} is greater than or equal to that day's threshold T_{max} and is one of at least three consecutive days experiencing T_{max} values above their own respective heatwave threshold T_{max} values.

Table S1. CMIP6 models and ensemble members

Model name	Ensemble members	Atmospheric resolution
ACCESS-CM2	r1i1p1f1, r2i1p1f1, r3i1p1f1	250 km
ACCESS-ESM1-5	r1i1p1f1, r2i1p1f1, r4i1p1f1, r5i1p1f1, r10i1p1f1	250 km
AWI-CM-1-1-MR	r1i1p1f1	100 km
CAMS-CSM1-0	r2i1p1f1	100 km
CanESM5	r10i1p1f1, r10i1p2f1, r11i1p1f1, r11i1p2f1, r12i1p1f1	100 km
CMCC-ESM2	r1i1p1f1	100 km
CNRM-CM6-1	r1i1p1f2	250 km
CNRM-CM6-1-HR	r1i1p1f2	100 km
CNRM-ESM2-1	r1i1p1f2	250 km
EC-Earth3	r1i1p1f1, r4i1p1f1, r11i1p1f1, r13i1p1f1, r15i1p1f1	100 km
EC-Earth3-Veg	r1i1p1f1, r4i1p1f1, r6i1p1f11	100 km
FGOALS-g3	r1i1p1f1, r3i1p1f1, r4i1p1f1	250 km
GFDL-CM4	r1i1p1f1	100 km
GFDL-ESM4	r1i1p1f1	100 km
GISS-E2-1-G[a]	r1i1p1f2	250 km
HadGEM3-GC31-MM	r1i1p1f3, r2i1p1f3, r3i1p1f3, r4i1p1f3	100 km
INM-CM4-8	r1i1p1f1	100 km
INM-CM5-0	r1i1p1f1	100 km
IPSL-CM6A-LR	r1i1p1f1, r2i1p1f1, r3i1p1f1, r4i1p1f1, r14i1p1f1	250 km
KACE-1-0-G	r1i1p1f1, r2i1p1f1	250 km
MIROC-ES2L	r1i1p1f2	500 km
MIROC6	r10i1p1f1, r11i1p1f1, r12i1p1f1, r13i1p1f1, r14i1p1f1	250 km
MPI-ESM1-2-HR	r1i1p1f1, r2i1p1f1	100 km
MPI-ESM1-2-LR	r1i1p1f1, r2i1p1f1, r3i1p1f1, r4i1p1f1, r10i1p1f1	250 km
MRI-ESM2-0	r1i1p1f1, r2i1p1f1, r4i1p1f1, r5i1p1f1	100 km
NESM3	r1i1p1f1	250 km
NorESM2-LM	r1i1p1f1	250 km
TaiESM1	r1i1p1f1	100 km
UKESM1-0-LL	r1i1p1f2, r2i1p1f2, r3i1p1f2, r4i1p1f2, r8i1p1f2	250 km

[a] Model only included in heatwave calculation and not in melt day analysis due to data availability.

References

Wilks, D. S. (2016). "The stippling shows statistically significant grid points": How research results are routinely overstated and overinterpreted, and what to do about it. *Bulletin of the American Meteorological Society*, *97*(12), 2263–2273. doi: 10.1175/BAMS-D-15-00267.1

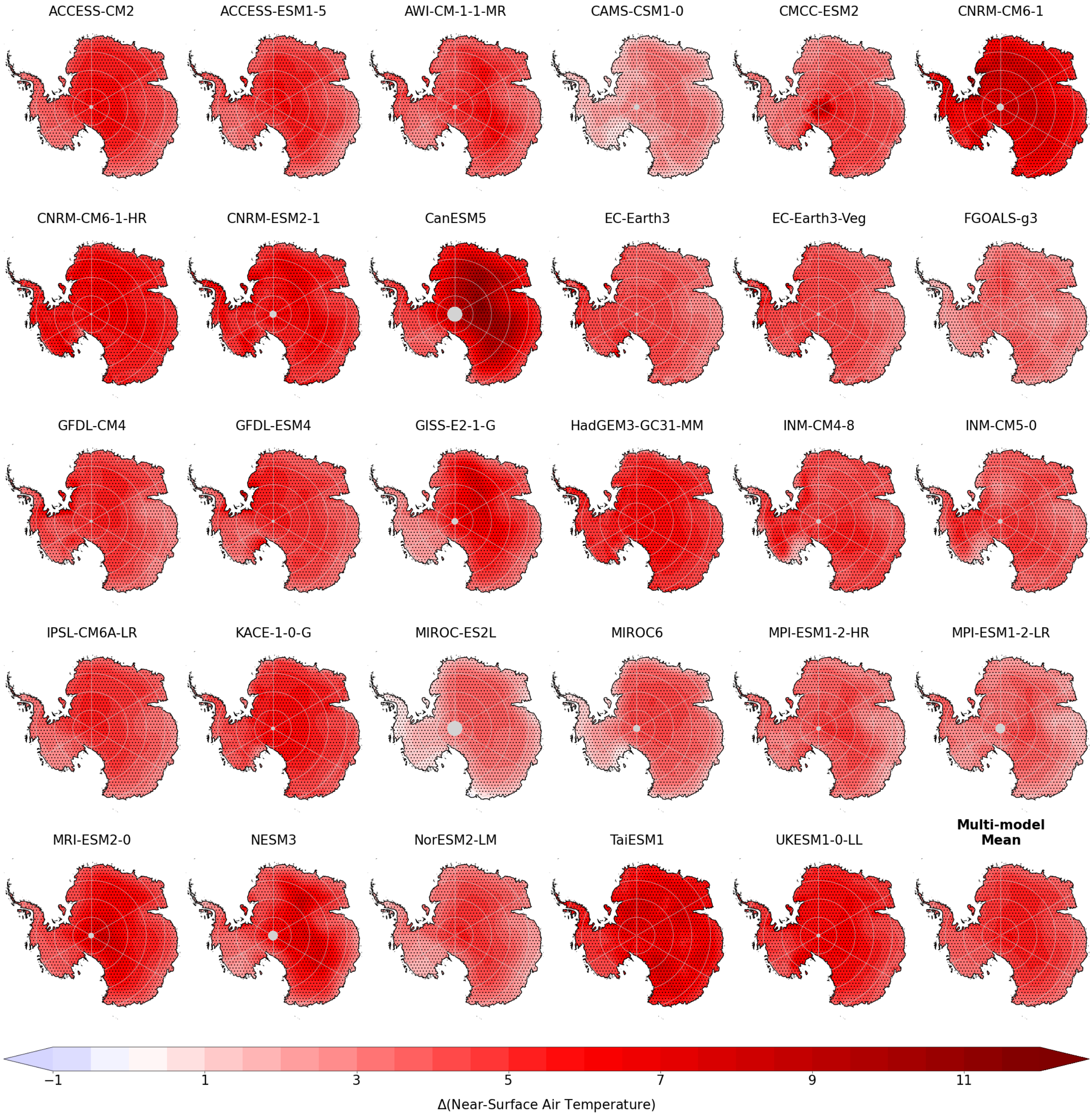

Figure S1. Change in CMIP6 models' ensemble member mean summer near-surface air temperature, 2070-2099 minus 1951-1980. The last panel is the CMIP6 multi-model mean. Stippling on each model's panel indicates where changes are statistically significant. Significance is determined using a Welch's t-test at every grid cell. Significance determinations are further limited for false discoveries using the recommendations made by Wilks (2016). We use an α_{FDR} of 0.10 to approximate a global significance level of 0.05. Stippling on the multi-model mean panel indicates where ≥80% of the CMIP6 models agree on the sign of the change.

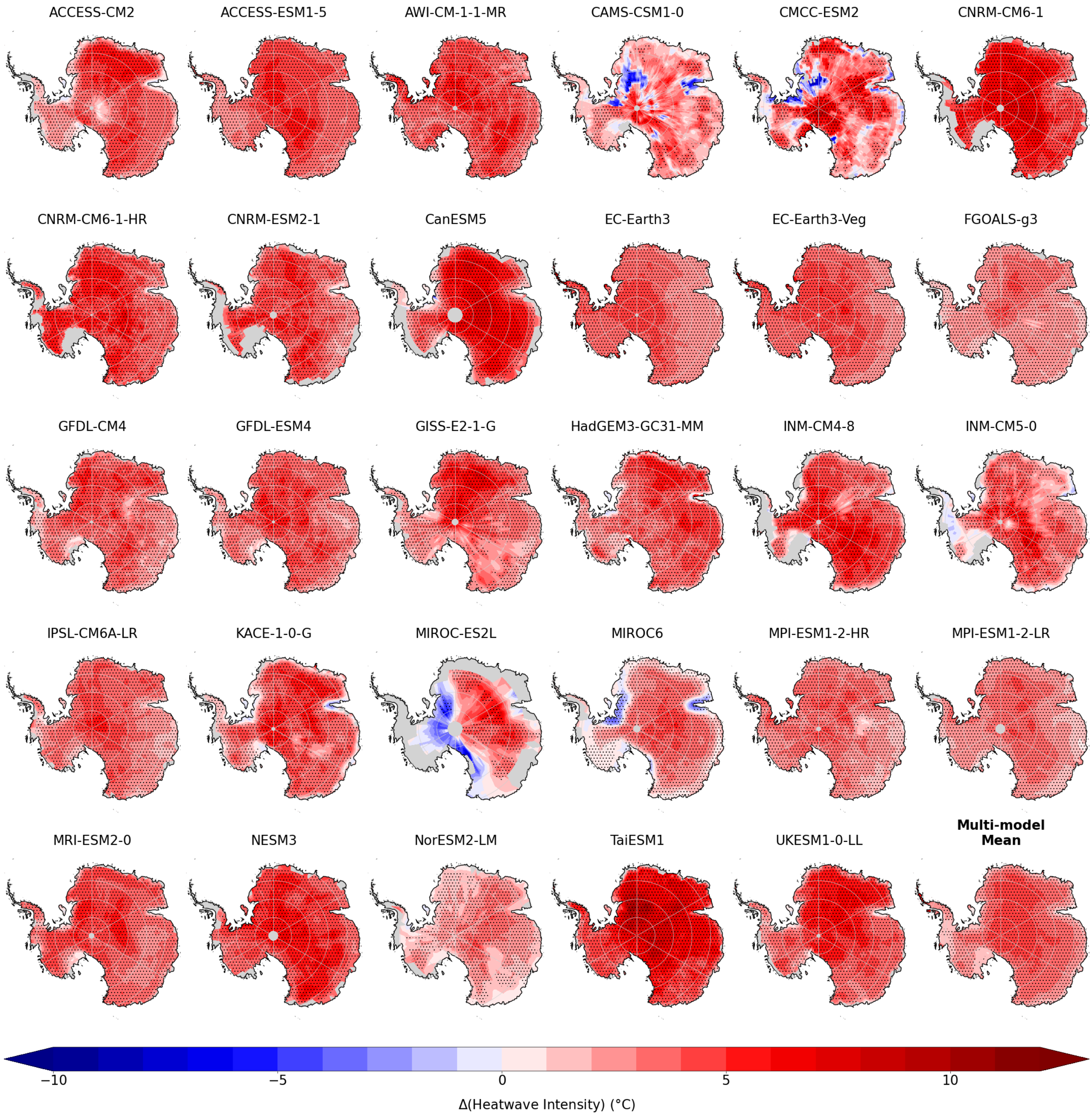

Figure S2. Change in CMIP6 models' ensemble member mean summer heatwave intensity, 2070-2099 minus 1951-1980. Intensity is the average heatwave temperature. The last panel is the CMIP6 multi-model mean. Stippling is as in Figure S1.

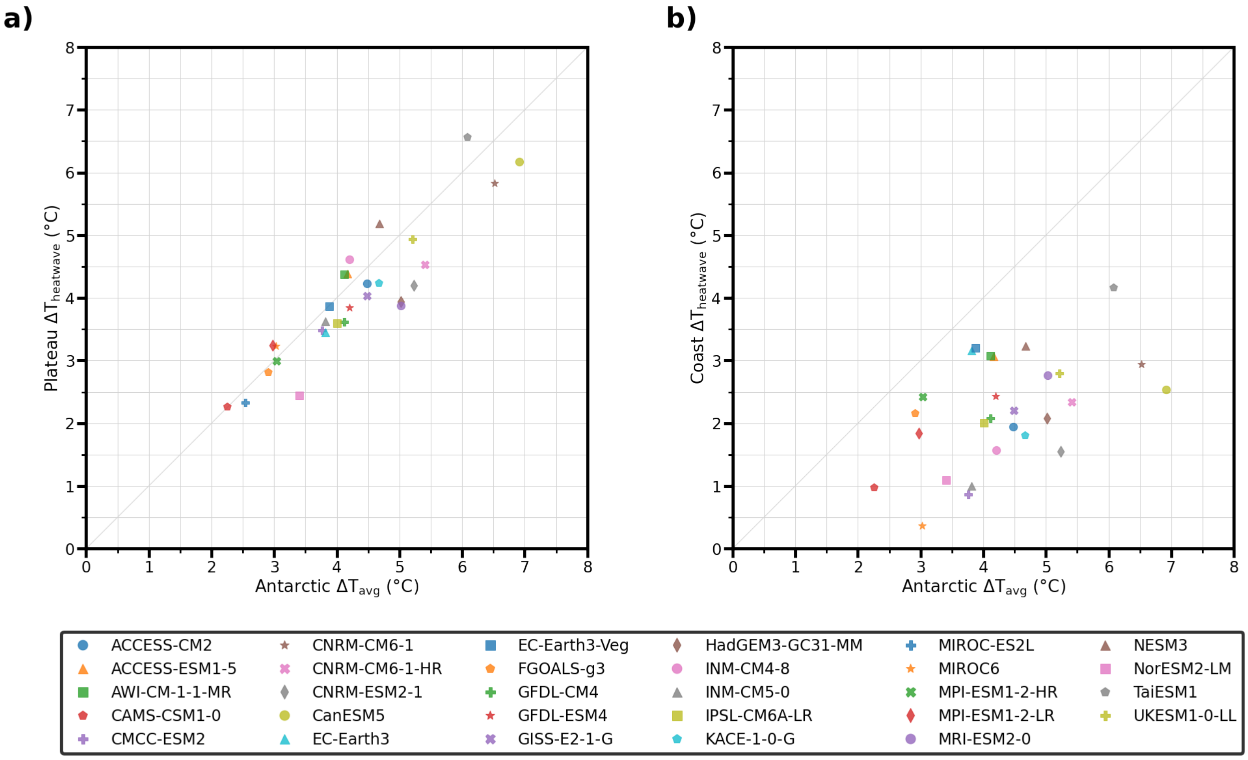

Figure S3. a) Scatterplot of change in CMIP6 models' summer heatwave intensity vs change in average daily near-surface air temperature over the East Antarctic Plateau (EAP), 2070-2099 minus 1951-1980. b) As in (a) except for over the non-EAP regions of Antarctica.

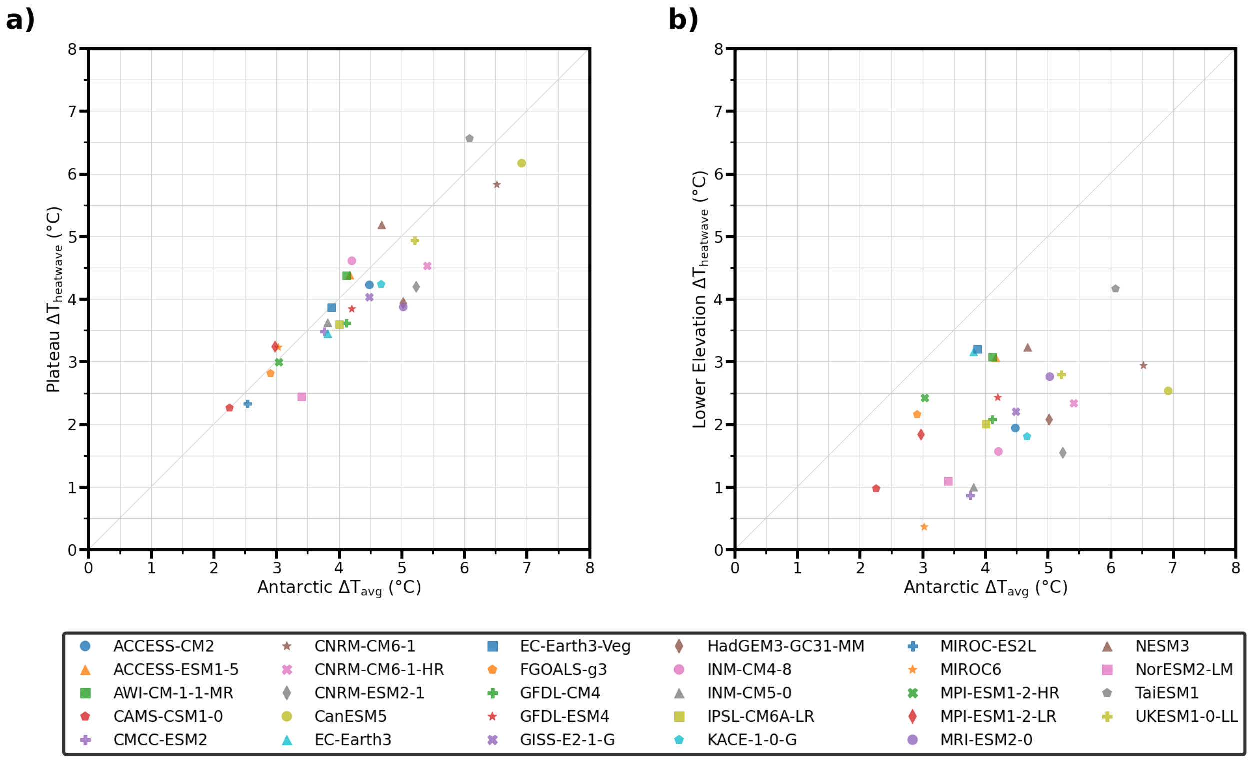

Figure S4. Change in CMIP6 models' ensemble member mean summer heatwave frequency, 2070-2099 minus 1951-1980. Frequency is the number of days that fall under heatwave conditions. The last panel is the CMIP6 multi-model mean. Stippling is as in Figure S1.

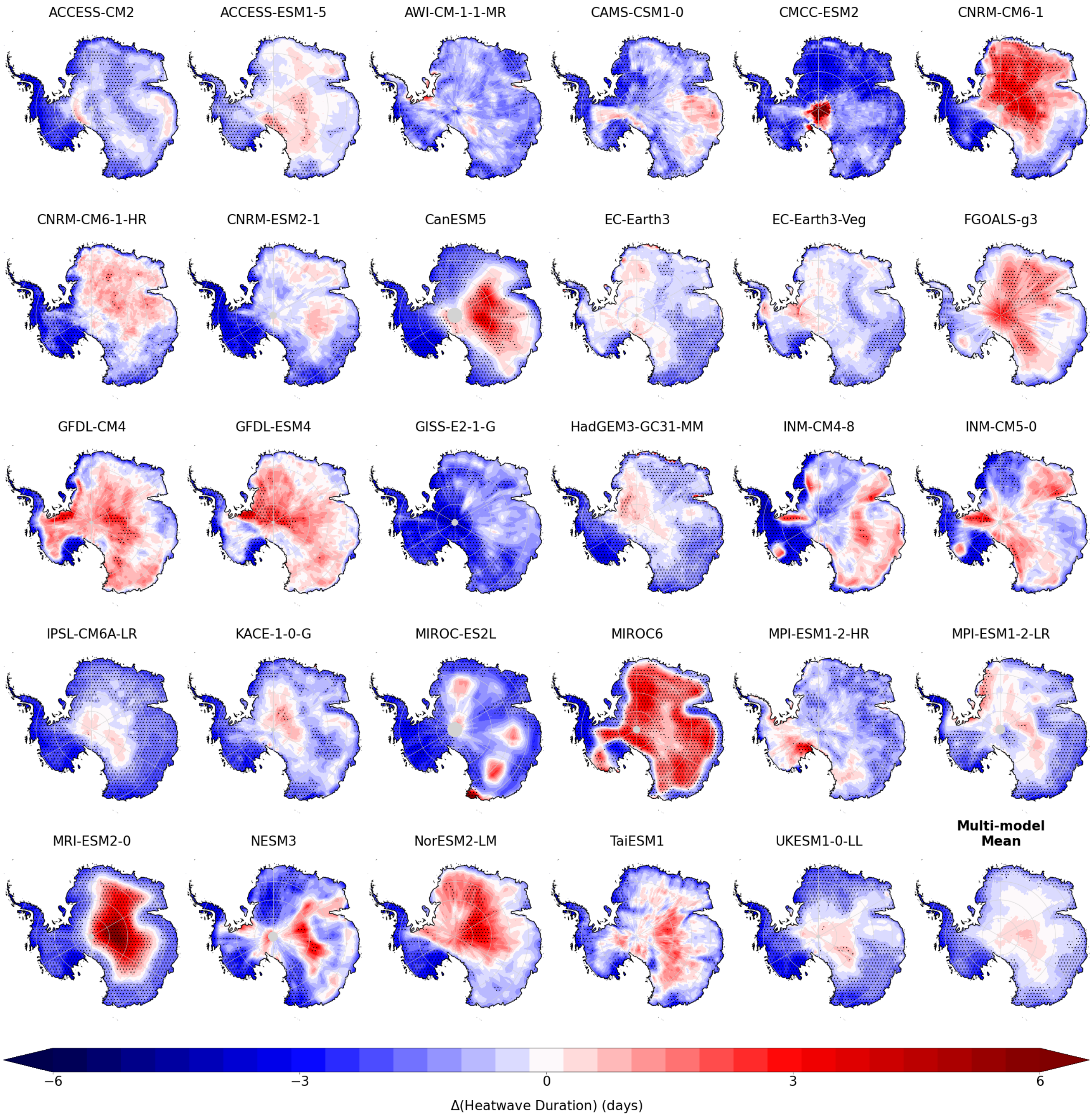

Figure S5. Change in CMIP6 models' ensemble member mean summer heatwave duration, 2070-2099 minus 1951-1980. A heatwave must last at least three days. The last panel is the CMIP6 multi-model mean. Stippling is as in Figure S1.

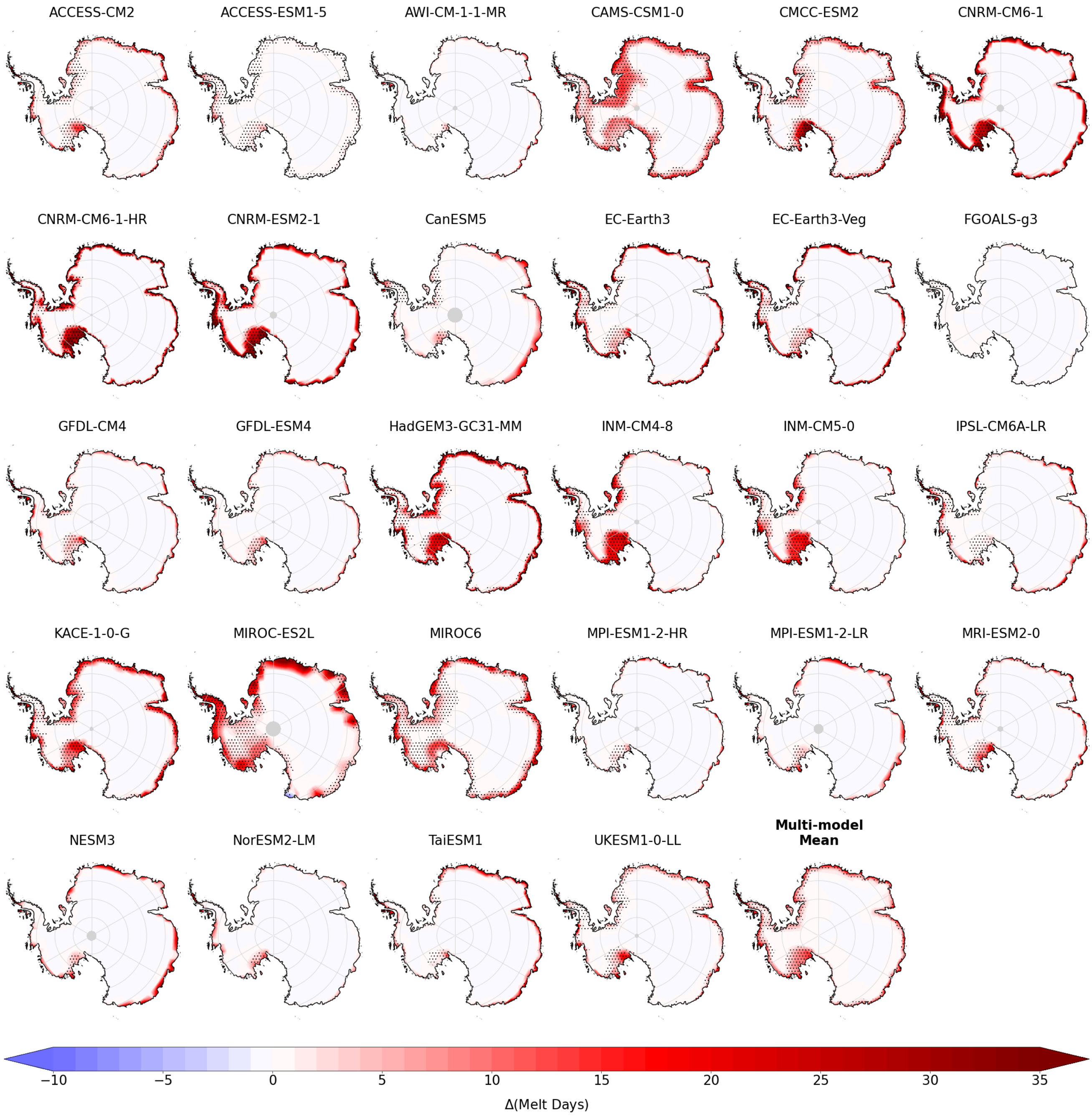

Figure S6. Change in CMIP6 models' ensemble member mean summer melt day frequency, 2070-2099 minus 1951-1980. The last panel is the CMIP6 multi-model mean. Stippling is as in Figure S1.

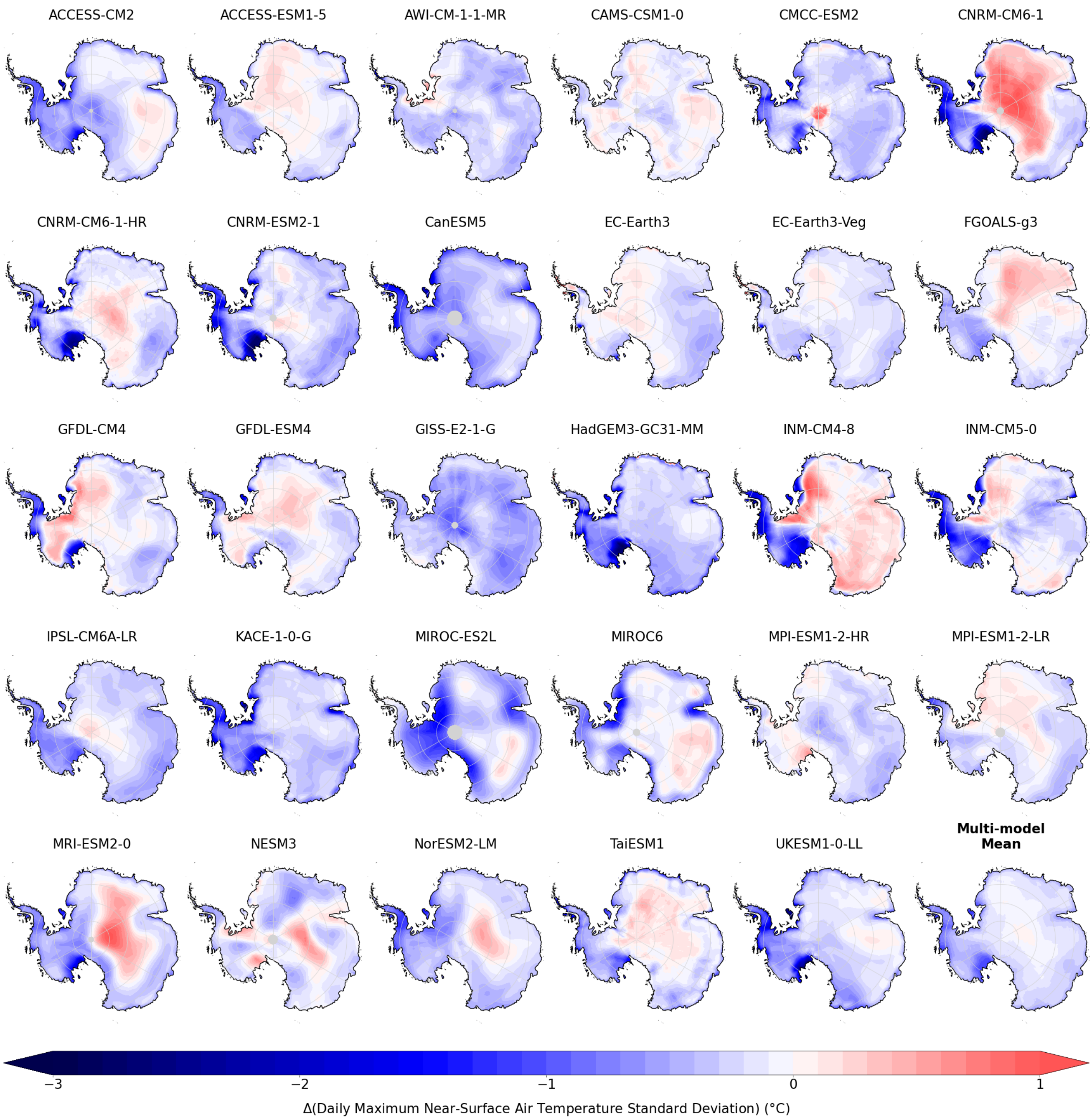

Figure S7. Change in CMIP6 models' ensemble member mean standard deviation of summer near-surface air temperature, 2070-2099 minus 1951-1980. The last panel is the CMIP6 multi-model mean.

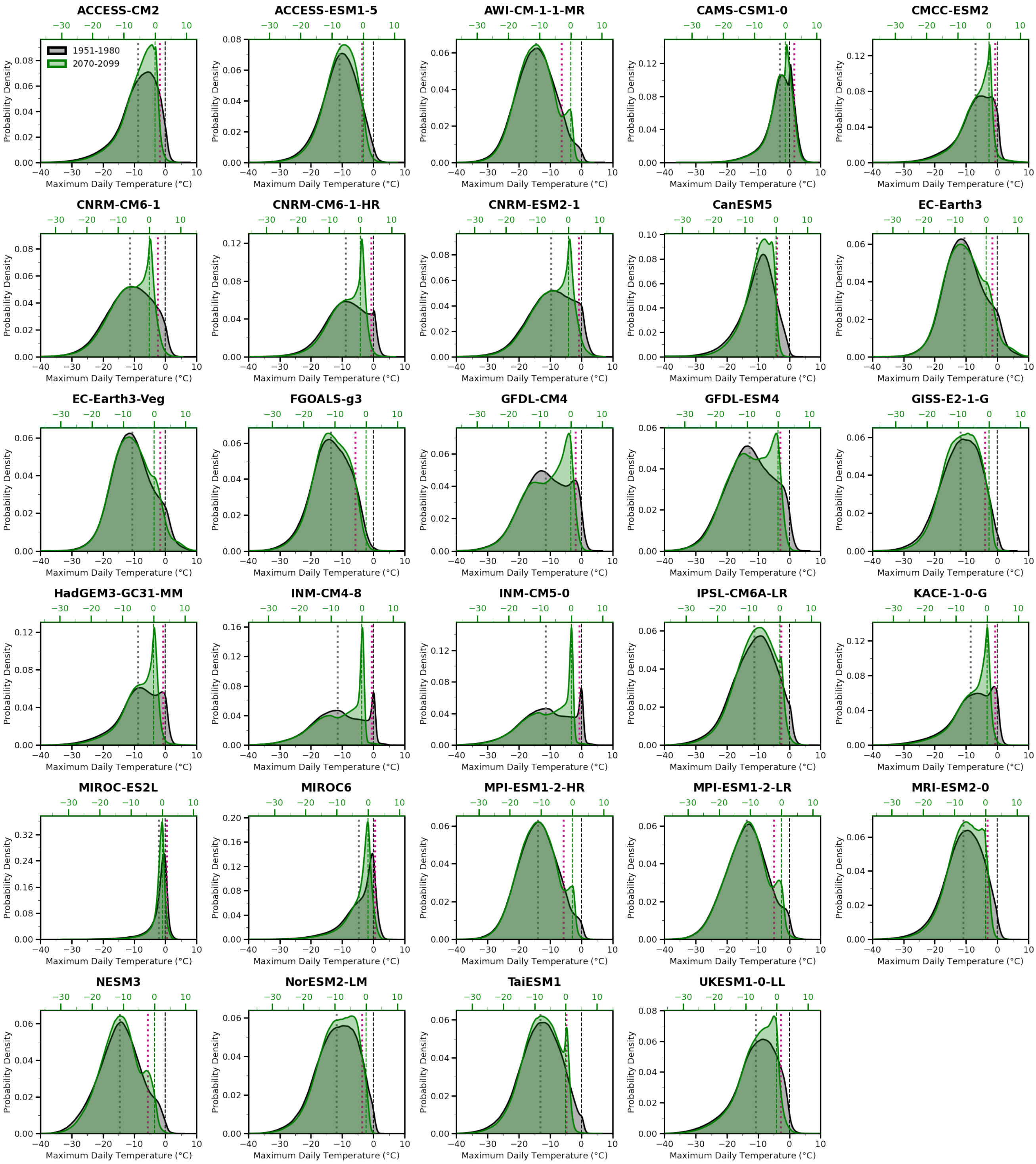

Figure S8. Probability distribution functions of non-EAP near-surface temperatures in CMIP6-participating ESMs, 1951-1980 (black) and 2070-2099 (green). The probability distribution functions are overlapped so the mean of each time period falls on the gray dotted line. The magenta dotted line is the 90th percentile of T_{max} during 1961-1980, or the threshold for calculating whether a day falls under heatwave conditions. The black (green) dashed line is the 0C threshold during 1951-1980 (2070-2099).